UC SANTA BARBARA

Recent results from CMS on Higgs boson properties

Ulascan Sarica
on behalf of
the CMS Collaboration

EPS 2021
26.07.2021

Synopsis

→ A selection of recent results from CMS on the Higgs boson properties measurements are summarized. The analyses are as follows with reference links:

- → Fiducial cross section measurements using $H \to \tau\tau$
  CMS-PAS-HIG-20-015
- → VH cross section using $H \to WW$ events
  CMS-PAS-HIG-19-017
- → Search for nonresonant $HH \to bb\gamma\gamma$
  CMS-HIG-19-018
- → Cross section and couplings measurement using $H \to \gamma\gamma$ events
  CMS-HIG-19-015
- → Cross section and couplings measurement using $H \to 4\ell$ events
  CMS-HIG-19-001
- → Anomalous HVV and Hff couplings using $H \to 4\ell$ events
  CMS-HIG-19-009

→ For more details on the specific analyses, you can find them in

> Jonathon's talk for cross section measurements in bosonic final states
> Andrew's talk for cross section measurements in fermionic final states
> Agni's talk for nonresonant and resonant HH searches
- See also the exciting $HH \to bbbb$ result in her talk from CMS-B2G-21-001.

Fiducial cross sections using $H \rightarrow \tau\tau$

→ Inclusive and differential measurements are reported.
  → Differential in p_T^H, p_T of leading jet, and jet multiplicity

→ Fiducial region definition:
  → Leptons include FSR within $\Delta R < 0.1$
  → $\mu\tau_h$: $p_T^{\mu} > 20$ GeV, $|\eta^{\mu}| < 2.1$, $p_T^{\tau_h} > 30$ GeV, $|\eta^{\tau_h}| < 2.3$, $m_T^{\ell} < 50$ GeV
  → $e\tau_h$: $p_T^{e} > 25$ GeV, $|\eta^{\mu}| < 2.1$, $p_T^{\tau_h} > 30$ GeV, $|\eta^{\tau_h}| < 2.3$, $m_T^{\ell} < 50$ GeV
  → $e\mu$: $p_T^{\ell_1\,(\ell_2\,)} > 24\ (15)$ GeV, $\left|\eta^{\ell}\right| < 2.4$, $\mathrm{m}_T^{\ell\ell} < 60$ GeV
  → $\tau_h\tau_h$: $p_T^{\tau_h} > 40$ GeV, $|\eta^{\tau_h}| < 2.1$, should have at least one jet
  → ~95% selection efficiency for $H \rightarrow \tau\tau$ with $\sigma_{fid}^{SM} = 408 \pm 27$ fb.

→ As Andrew mentioned, event categorization improved wrt. prior studies as
  → $\ell\tau_h$: $p_T^{\tau_h}$ within [30 GeV, 50 GeV], [50 GeV, 70 GeV], or $>$ 70 GeV
  → $\tau_h\tau_h$: Subleading $p_T^{\tau_h}$ within [40 GeV, 50 GeV], [50 GeV, 70 GeV], or $>$ 70 GeV
    → Based on changes in mis-id rate
  → $e\mu$: Kept inclusive

→ Fits are performed using $m_{\tau\tau}$ and the differential variable of interest with 2D histograms.

Fiducial cross sections using $H \rightarrow \tau\tau$

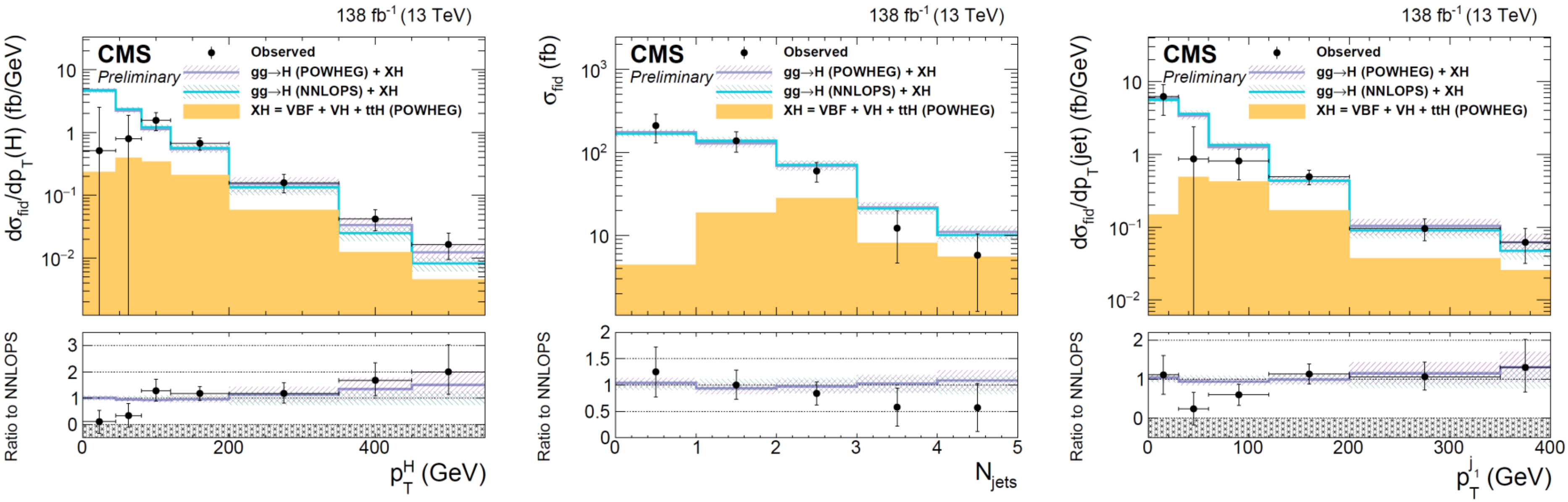

→ As a reminder from Andrew's slides, the observed and expected fiducial differential cross sections are as above in bins of the variables of interest.

→ The inclusive cross section is measured to be 426 ± 102 fb, consistent with $\sigma_{fid}^{SM} = 408 \pm 27$ fb.

Fiducial cross sections using $H \rightarrow \tau\tau$

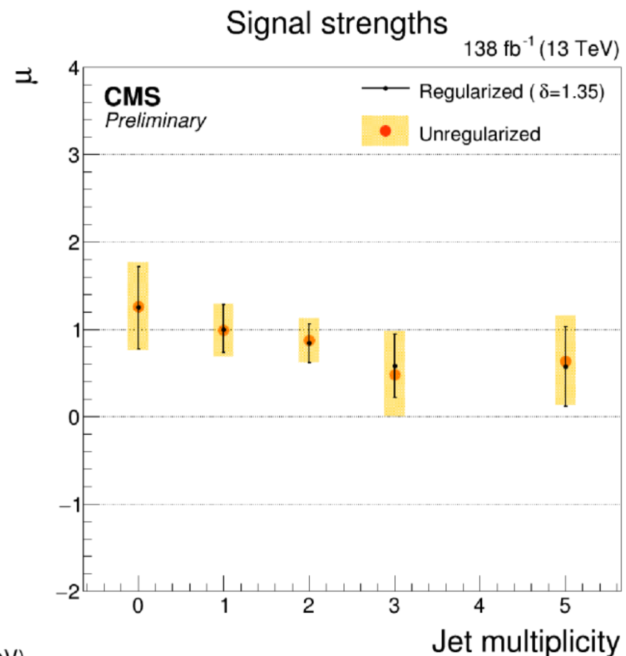

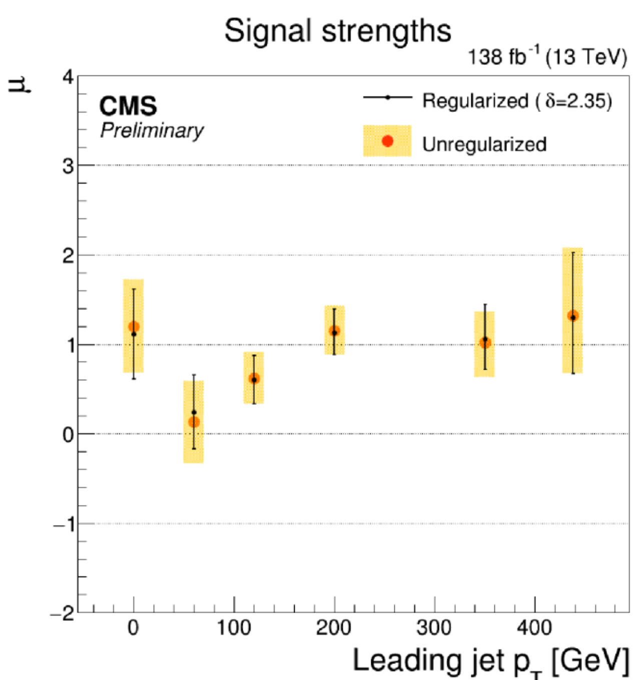

→ 'Regularized' refers to a Tikhonov procedure to mitigate statistical fluctuations in unfolding. (see Andrew's talk for the procedure)

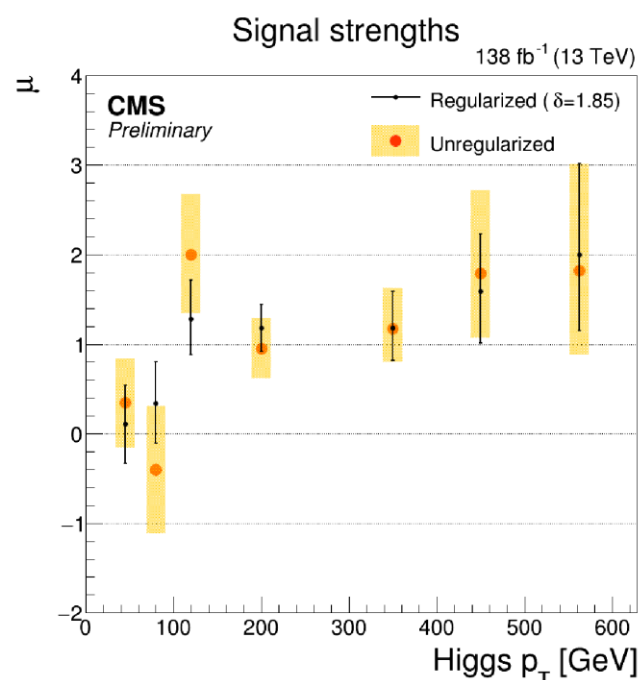

VH cross section using $H \to WW$

→ Events from the $WH \to 2\ell 2\nu qq$ (same-sign leptons, $WHSS$), $WH \to 3\ell 3\nu$ ($WH3\ell$), $ZH \to 3\ell\nu qq$ ($ZH3\ell$), and $ZH \to 4\ell 2\nu$ ($ZH4\ell$) are combined.

→ Measurement is done both inclusively and in bins of p_T^V: 0-150 GeV, and > 150 GeV:

→ Inclusive measurement assumes relative ratio of different production mechanisms are as in the SM.

→ Differential measurement done with the ratio ZH/WH unconstrained or fixed to the SM expectation.

→ The final observables used in the fit are either an approximation to m_H ($WHSS$ and $ZH3\ell$), or a BDT discriminant ($WH3\ell$ and $ZH4\ell$). The elements of event selection are optimized in each channel to reduce backgrounds, but the main orthogonality condition is as follows:

	WHSS	WH3l	ZH3l	ZH4l
Number of leptons with $p_T > 10$ GeV	2	3	3	4
Number of jets with $p_T > 30$ GeV	≥ 1	0	≥ 1	—

VH cross section using $H \to WW$

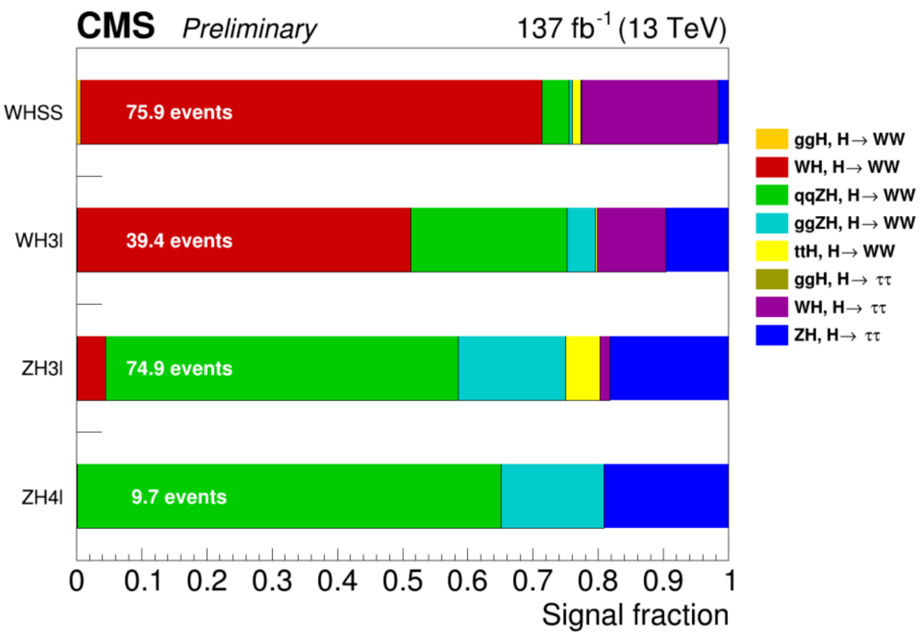

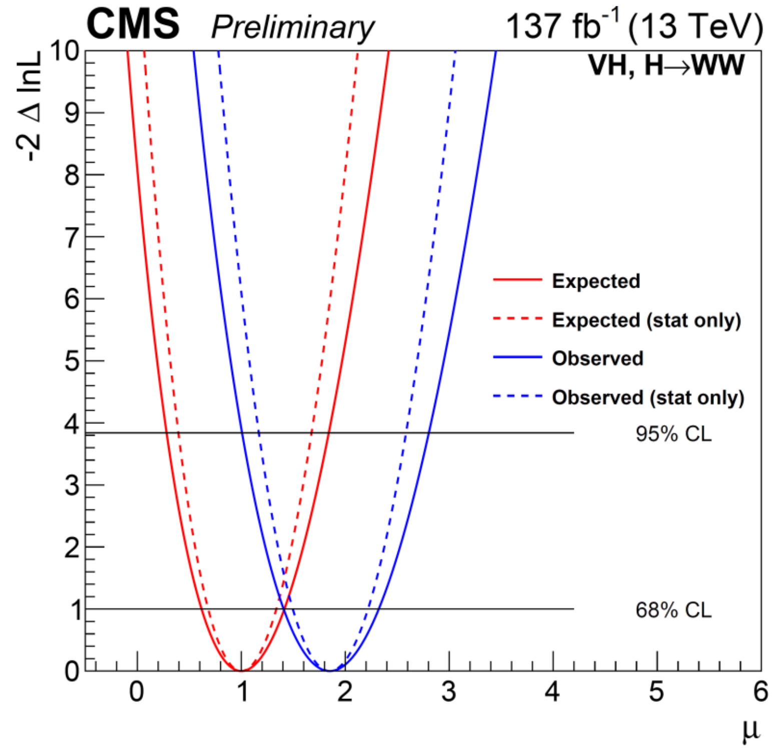

For the inclusive measurement, the signal composition is shown on the top left, and the profiled likelihood scan for the fitted μ is on the top right.

→ The combined best-fit value is

$\mu = 1.85^{+0.33}_{-0.32}$ (stat.) $^{+0.27}_{-0.25}$ (exp.) $^{+0.10}_{-0.07}$ (th.)

→ Results from individual channels is on this table.

Category	μ	Significance
WHSS	$0.95^{+0.94}_{-0.96}$	1.0 σ (1.1 σ expected)
WH3l	$2.20^{+0.86}_{-0.79}$	3.0 σ (1.6 σ expected)
ZH3l	$4.12^{+1.73}_{-1.68}$	2.5 σ (0.6 σ expected)
ZH4l	$1.73^{+0.75}_{-0.65}$	3.1 σ (2.1 σ expected)
Combination	$1.85^{+0.47}_{-0.44}$	4.7 σ (2.8 σ expected)

VH cross section using $H \rightarrow WW$

	μ	Significance
$WH\ p_{\mathrm{T}}^{\mathrm{V}} < 150$ GeV	$1.5^{+1.0}_{-0.9}$	1.64 σ (1.24 σ expected)
$WH\ p_{\mathrm{T}}^{\mathrm{V}} > 150$ GeV	$3.6^{+1.8}_{-1.6}$	2.23 σ (0.83 σ expected)
$ZH\ p_{\mathrm{T}}^{\mathrm{V}} < 150$ GeV	$3.4^{+1.1}_{-1.0}$	4.37 σ (1.59 σ expected)
$ZH\ p_{\mathrm{T}}^{\mathrm{V}} > 150$ GeV	$0.8^{+1.2}_{-0.9}$	0.83 σ (1.18 σ expected)

→ For the differential measurement, results of fits to the signal strength modifiers with separate WH and ZH parameters are given as above.

→ Results with ZH/WH fixed to the SM prediction are

$\mu_{p_T^V<150\ \mathrm{GeV}} = 2.65^{+0.57}_{-0.55}$ (stat.) $^{+0.38}_{-0.32}$ (exp.) $^{+0.08}_{-0.07}$ (th.)

$\mu_{p_T^V>150\ \mathrm{GeV}} = 1.56^{+0.85}_{-0.77}$ (stat.) $^{+0.43}_{-0.40}$ (exp.) $^{+0.11}_{-0.09}$ (th.)

Nonresonant HH in the $bb\gamma\gamma$ final state

→ Analysis is published in JHEP 03 (2021) 257.

→ One of the most sensitive to HH due to large $BR(H \to b\bar{b})$ and good mass resolution in $H \to \gamma\gamma$.

→ Event selection and categorization targets gg and VBF production using MVA discrimnants.

→ Constraints are derived in terms of $\sigma_{HH} \cdot BR(HH \to \gamma\gamma\mathrm{b\bar{b}})$, and coupling modifiers κ_λ, κ_t, and c_{2V}.
→ Results combine with $t\bar{t}H, H \to \gamma\gamma$ (CMS-HIG-19-013), which enables simultaneous constraints on κ_λ and κ_t.
→ A few BSM benchmarks are also considered.

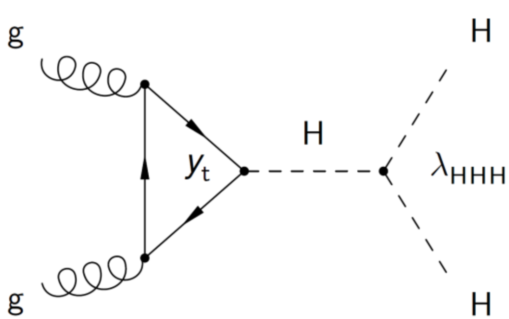

$\sim\kappa_\lambda$

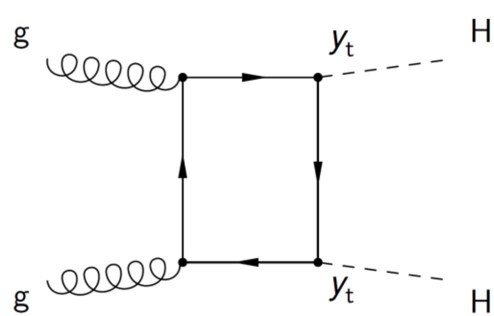

$\sim\kappa_t$

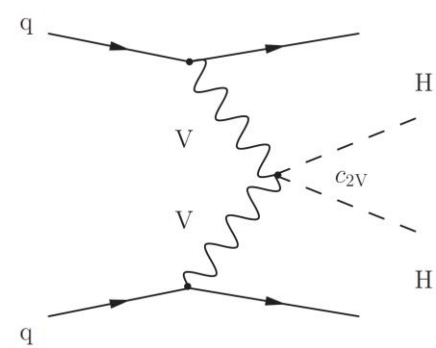

c_{2V}

Nonresonant HH in the $bb\gamma\gamma$ final state

→ Two separate MVA discriminants are used in distinguishing gg and VBF events against the dominant $\gamma\gamma$+jets and γ+jets backgrounds:
→ The discriminants use kinematic observables related to the Higgs candidates, helicity angles, jet kinematics, b- or quark/gluon-tagging, or other kinematic variables related to the HH system.

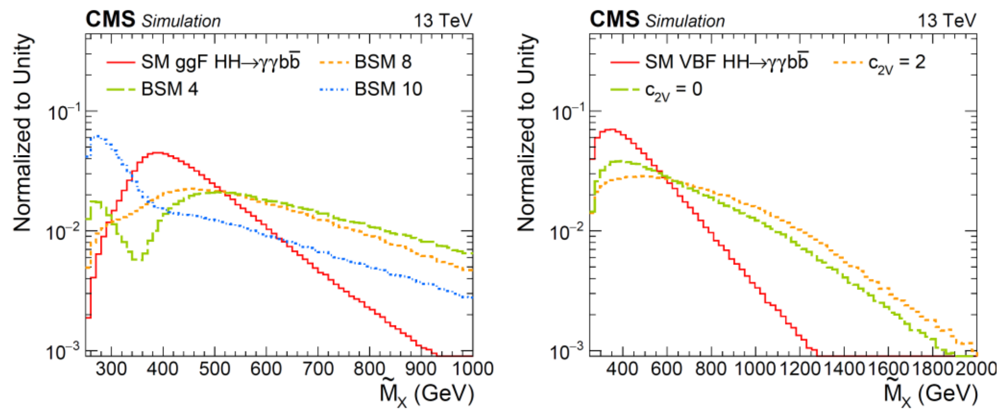

→ The quantity $\widetilde{M}_X$ is sensitive to the BSM benchmarks and the different c_{2V} values, so it is included as part of the categorization:

$$\widetilde{M}_{\mathrm{X}} = m_{\gamma\gamma\mathrm{jj}} - (m_{\mathrm{jj}} - m_{\mathrm{H}}) - (m_{\gamma\gamma} - m_{\mathrm{H}})$$

Category	MVA	$\widetilde{M}_{\mathrm{X}}$ (GeV)
VBF CAT 0	0.52–1.00	>500
VBF CAT 1	0.86–1.00	250–500
ggF CAT 0	0.78–1.00	>600
ggF CAT 1		510–600
ggF CAT 2		385–510
ggF CAT 3		250–385
ggF CAT 4	0.62–0.78	>540
ggF CAT 5		360–540
ggF CAT 6		330–360
ggF CAT 7		250–330
ggF CAT 8	0.37–0.62	>585
ggF CAT 9		375–585
ggF CAT 10		330–375
ggF CAT 11		250–330

→ The final categorization is done using a combination of the two discriminants and the range of $\widetilde{M}_X$. The fits are performed on $m_{\gamma\gamma}$ and m_{jj} as observables.

→ See also Agni's talk for more details on HH results.

Nonresonant HH in the $bb\gamma\gamma$ final state

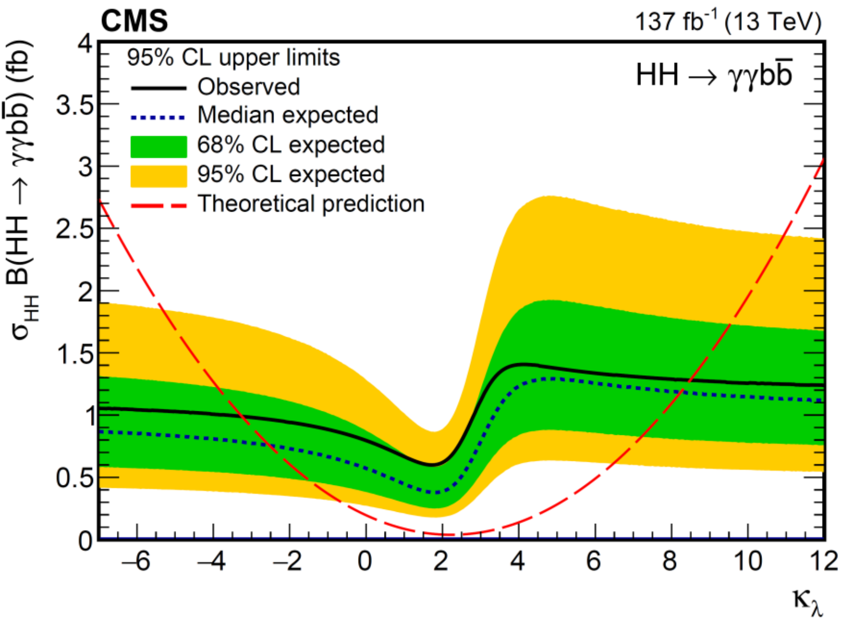

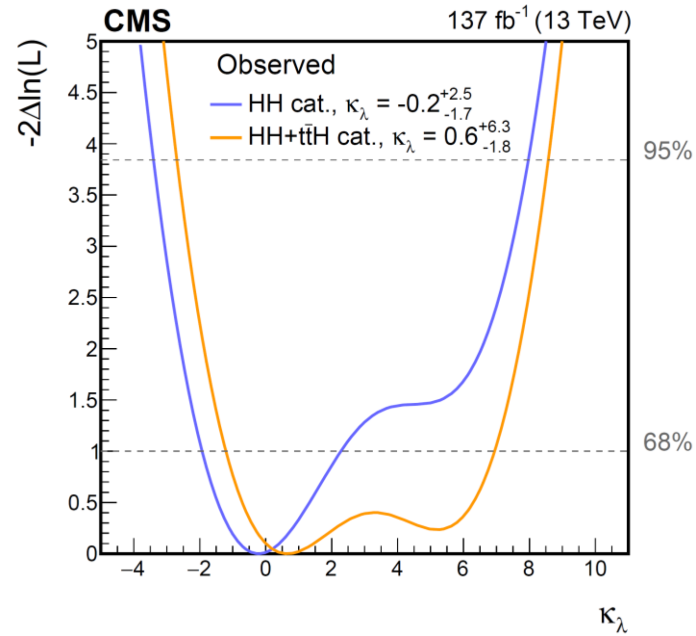

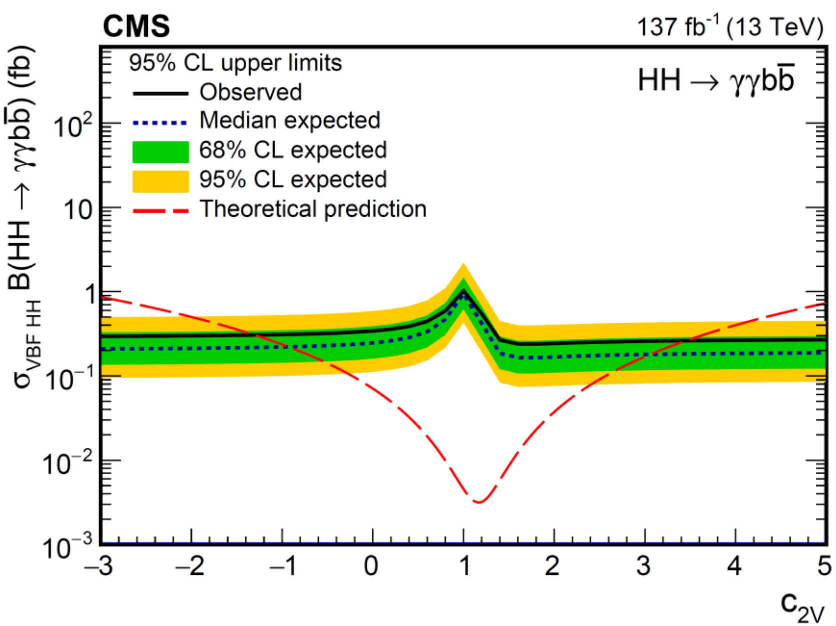

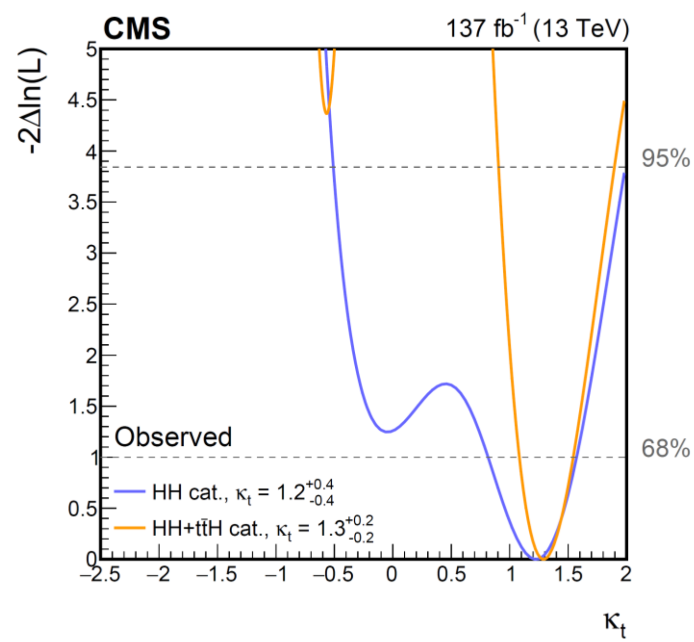

Cross sections and couplings using $H \to \gamma\gamma$

→ Analysis is published in JHEP 07 (2021) 027.

→ Event categorization targets optimal selection for the STXS framework. Most of the event categories are constructed using BDTs that are able to parallel the STXS 1.2 bin classification.

→ Measurements are done for the signal strength modifiers, the STXS 1.2 cross sections merged using two different scenarios, or a few κ parameters under different assumptions.
→ Merging needs to be considered in STXS bins in order to avoid very large uncertainties or correlations.
→ In the maximal merging scheme (17 bins), the bins are merged until the expected uncertainties are less than 150% of the SM prediction.
→ In the minimal scheme (27 bins), the merging requires correlations to be less than 90%.

→ An observed (expected) upper limit of $\mu_{tH} < 14\ (8)$ is also placed.

Cross sections and couplings using $H \rightarrow \gamma\gamma$

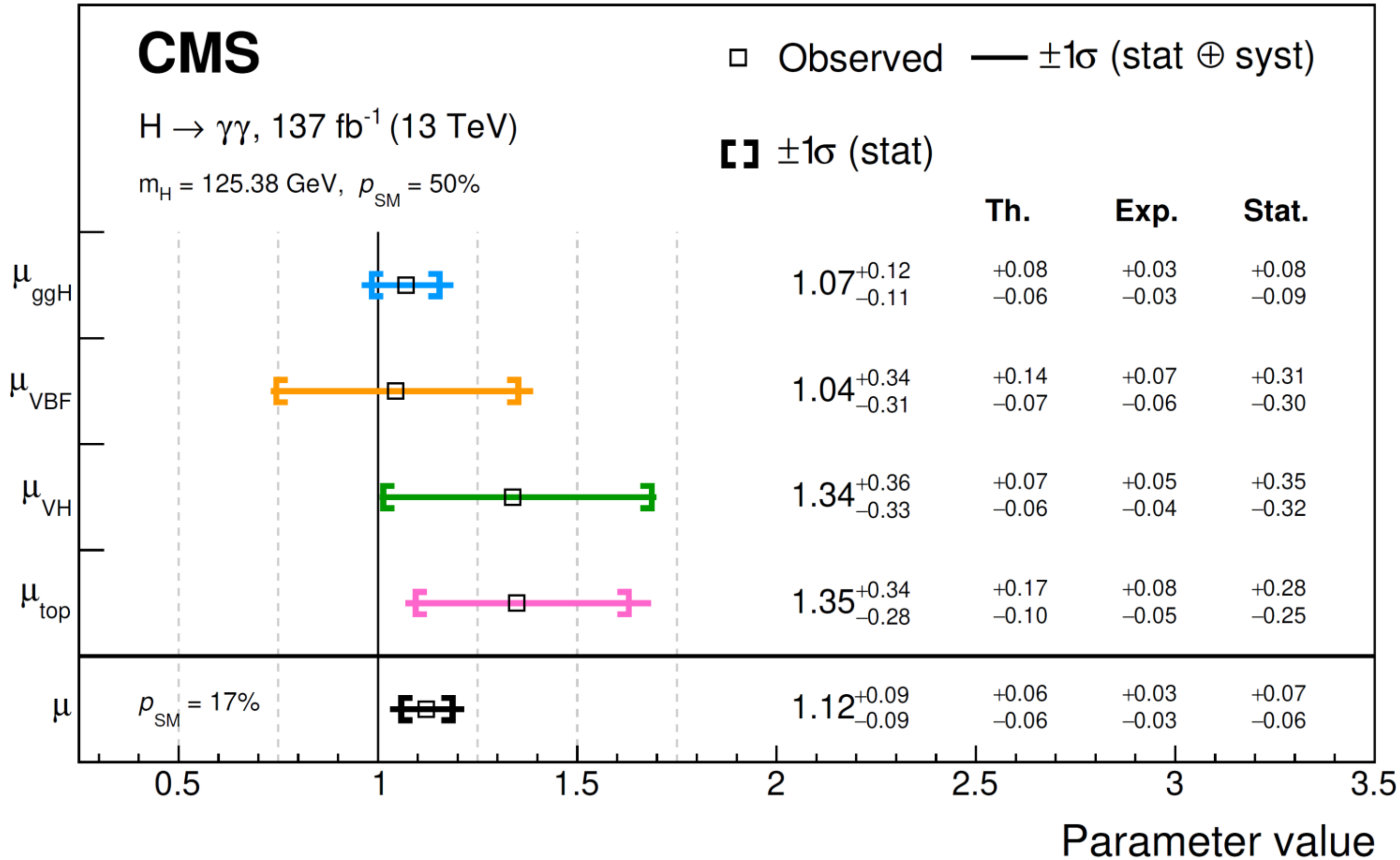

→ Signal strength modifiers are parametrized for ggH, VBF, VH, and the processes that include associated top quarks.

→ Improvements from past analyses come from the increase in luminosity but also the improvements in the analysis technique.

Cross sections and couplings using $H \to \gamma\gamma$

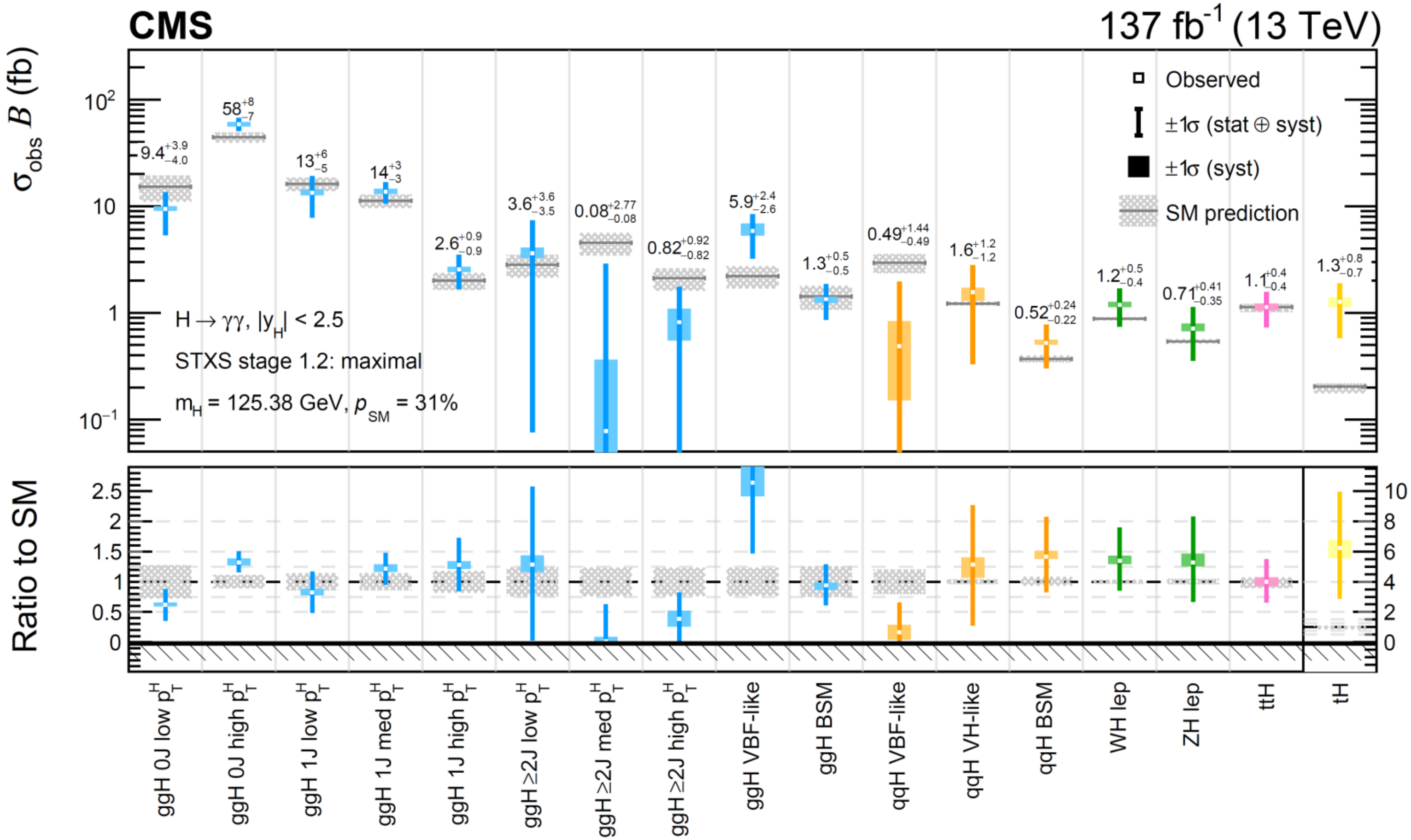

→ Results shown are for the maximal merging scheme.

Cross sections and couplings using $H \rightarrow \gamma\gamma$

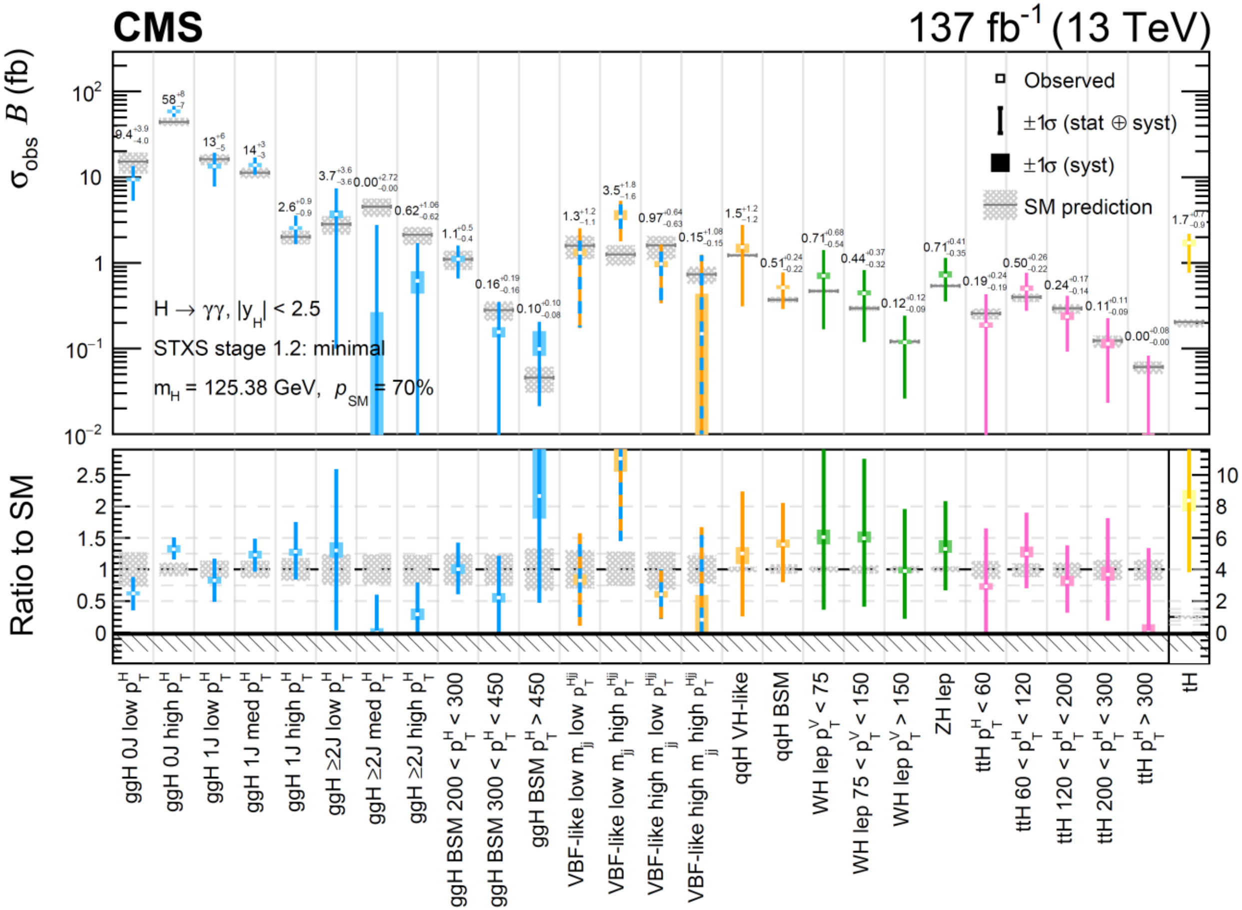

→ Results shown are for the minimal merging scheme.

Cross sections and couplings using $H \rightarrow \gamma\gamma$

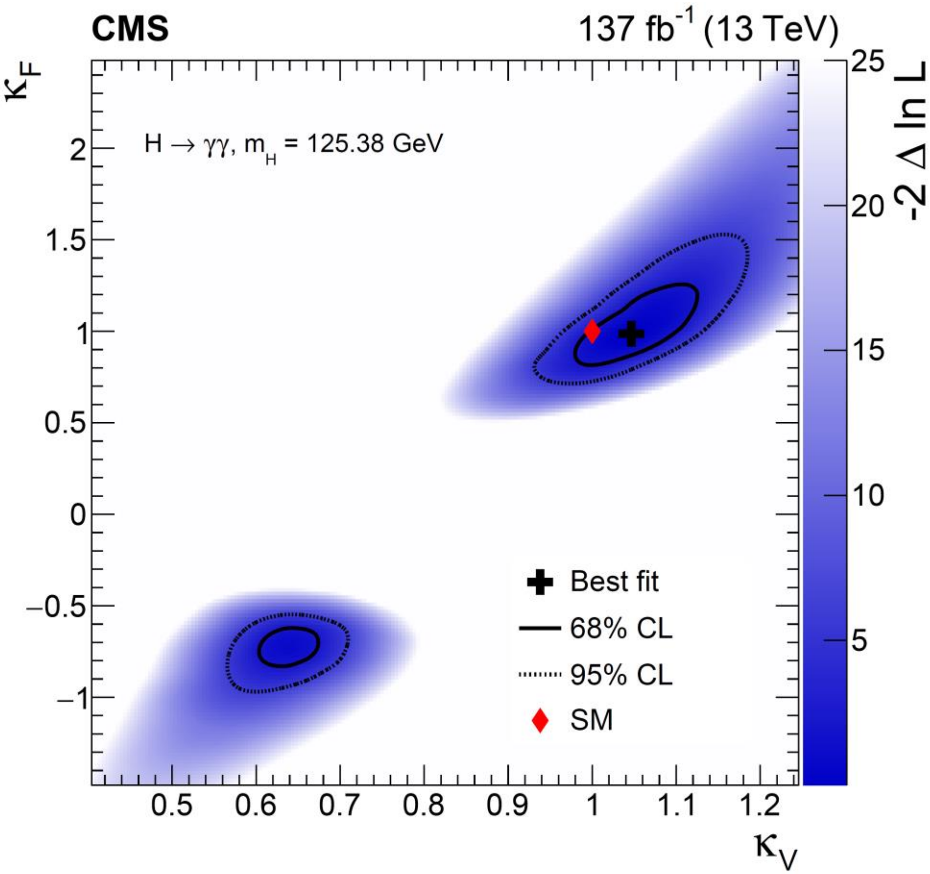

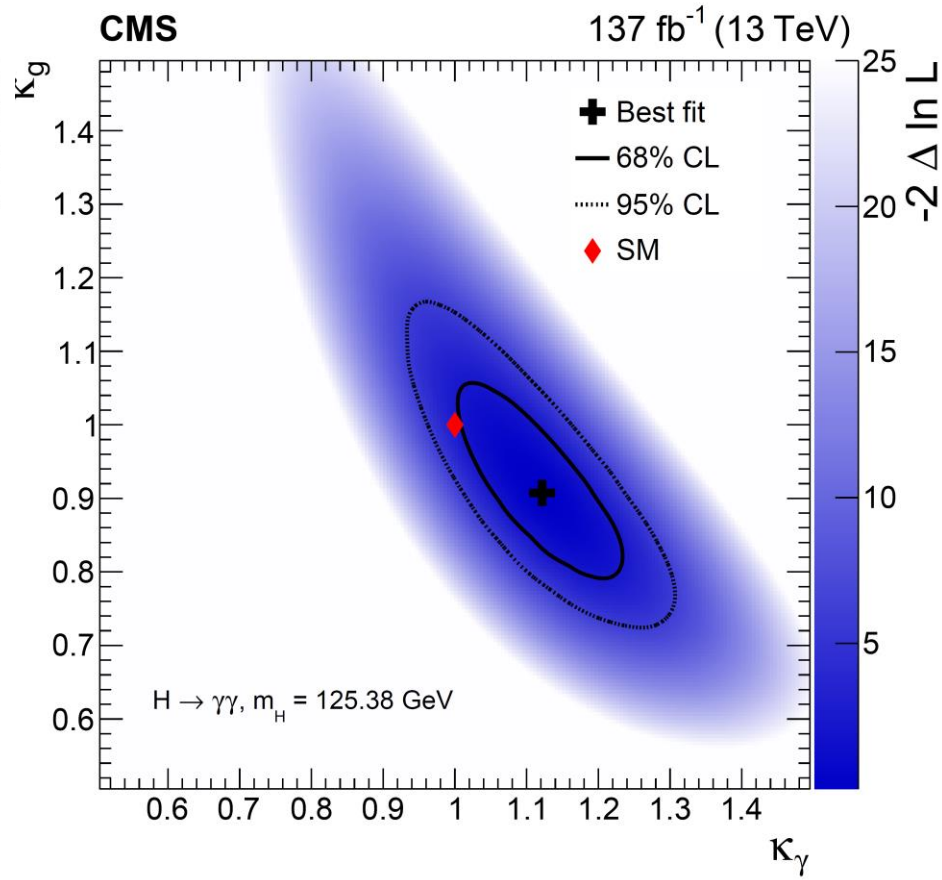

→ Resolved model disambiguates the fermionic and bosonic coupling contributions in $H \rightarrow \gamma\gamma$, $gg \rightarrow ZH$, tH, and tHW, including the interference terms.

→ Unresolved model keeps $gg \rightarrow H$ and $H \rightarrow \gamma\gamma$ separated with other κ parameters fixed at 1.

Cross sections and couplings using $H \to 4\ell$

→ Analysis is published in EPJC 81 (2021) 488.

→ The analysis measures signal strength modifiers and $\sigma \cdot BR$ values in the STXS Stage 0 and Stage 1.2 bins, and provides inclusive and differential fiducial cross section measurements.
→ Results provided for the STXS 1.2 bins merge bins to reduce large uncertainties and correlations.

→ Event categorization, observables, and the choice of the $ZZ \to 4\ell$ candidate when there are > 4 leptons make extensive use of MELA matrix element discriminants.
→ A two-level categorization is performed targeting STXS Stage 0, and the further splitting to also target STXS Stage 1.2.
→ The first level tags for VBF (≥ 2 jets), VBF (1 jet), and hadronic and leptonic VH or $t\bar{t}H$ categories with the rest being untagged.
→ The second level splits the events further in p_T^{4l}, p_T^{4l+jj}, or m_{jj}.

→ The use of D_{bkg}, which discriminates $H \to 4\ell$ processes against background, in $ZZ \to 4\ell$ candidate choice and the set of observables is dropped when fiducial cross section measurements are performed to reduce model dependence. A definition of the fiducial region can be found in the paper.

Cross sections and couplings using $H \rightarrow 4\ell$

	Expected	Observed
$\mu_{t\bar{t}H,tH}$	$1.00^{+1.23}_{-0.77}$ (stat) $^{+0.51}_{-0.06}$ (syst)	$0.17^{+0.88}_{-0.17}$ (stat) $^{+0.42}_{-0.00}$ (syst)
μ_{WH}	$1.00^{+1.83}_{-1.00}$ (stat) $^{+0.75}_{-0.00}$ (syst)	$1.66^{+1.52}_{-1.66}$ (stat) $^{+0.85}_{-0.00}$ (syst)
μ_{ZH}	$1.00^{+4.79}_{-1.00}$ (stat) $^{+6.76}_{-0.00}$ (syst)	$0.00^{+4.38}_{-0.00}$ (stat) $^{+3.24}_{-0.00}$ (syst)
μ_{VBF}	$1.00^{+0.53}_{-0.44}$ (stat) $^{+0.18}_{-0.12}$ (syst)	$0.48^{+0.46}_{-0.37}$ (stat) $^{+0.14}_{-0.10}$ (syst)
$\mu_{ggH,b\bar{b}H}$	1.00 ± 0.10 (stat) $^{+0.12}_{-0.10}$ (syst)	0.99 ± 0.09 (stat) $^{+0.11}_{-0.09}$ (syst)
μ	$1.00^{+0.08}_{-0.07}$ (stat) $^{+0.10}_{-0.08}$ (syst)	0.94 ± 0.07 (stat) $^{+0.09}_{-0.08}$ (syst)

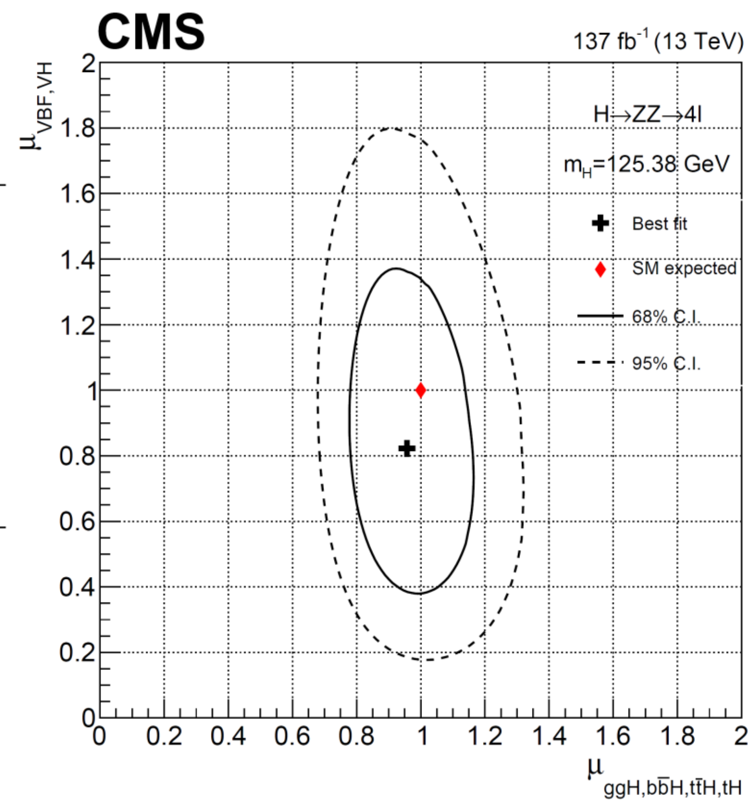

→ Results interpreted in terms of signal strength parameters are grouped for each production mechanism, or those that contain Hff couplings vs not.

→ A 2-parameter profiled likelihood is provided for the latter as shown on the right.

Cross sections and couplings using $H \rightarrow 4\ell$

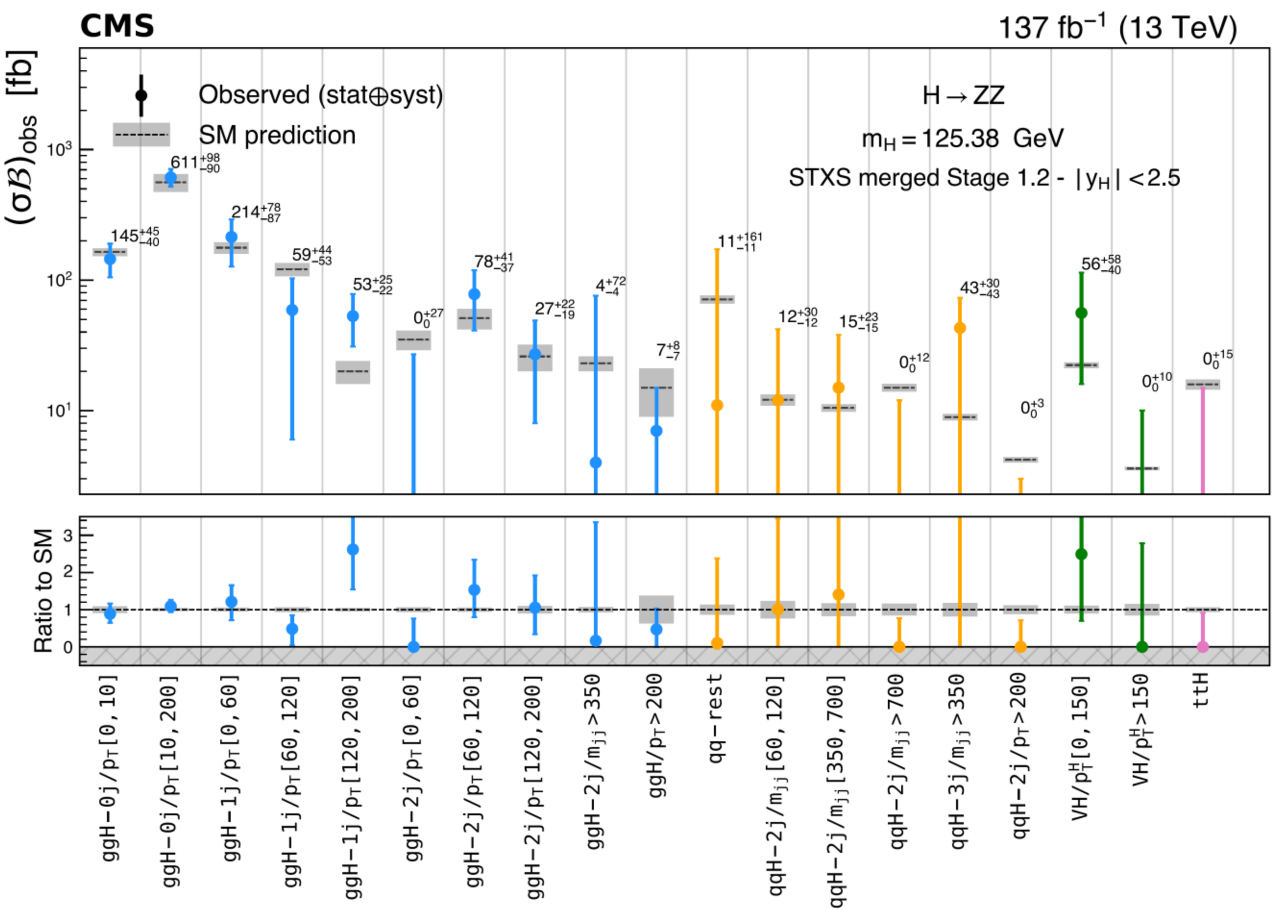

→ Results are presented for a merged set of STXS 1.2 bins.

→ A set of STXS Stage 0 measurements can also be found in the paper.

Cross sections and couplings using $H \rightarrow 4\ell$

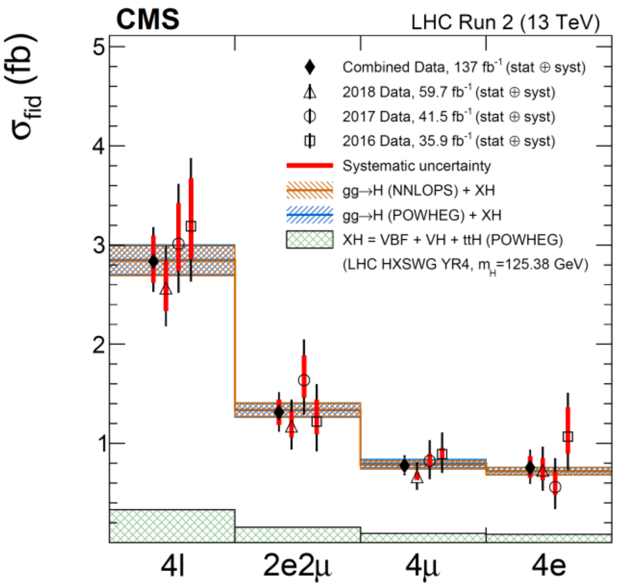

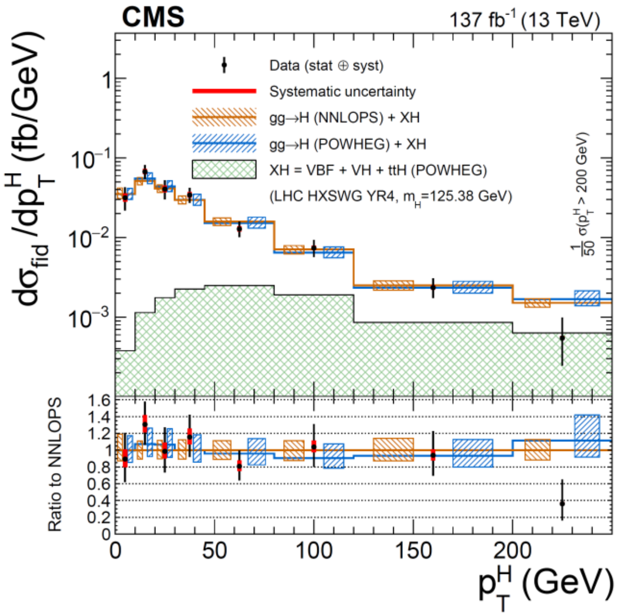

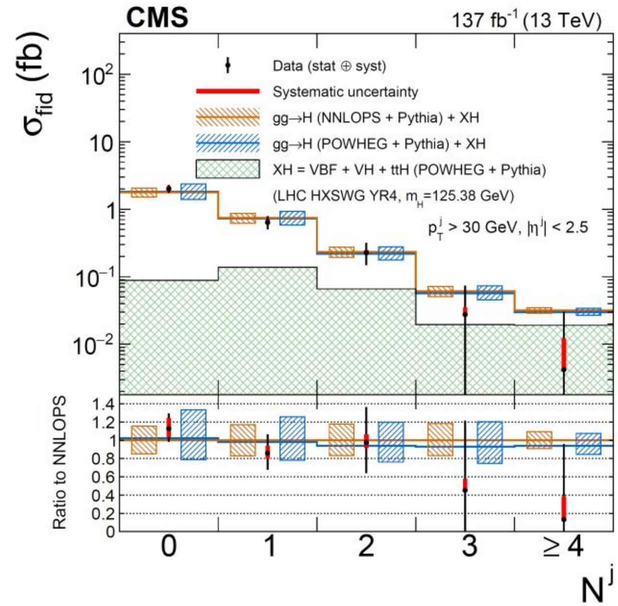

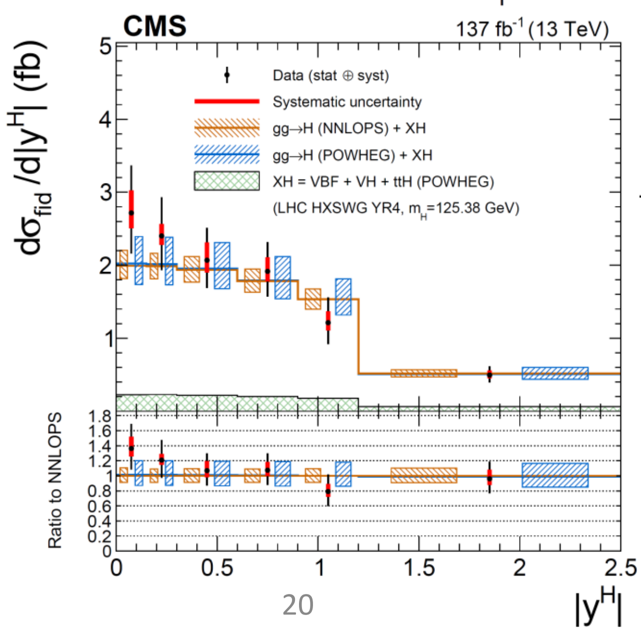

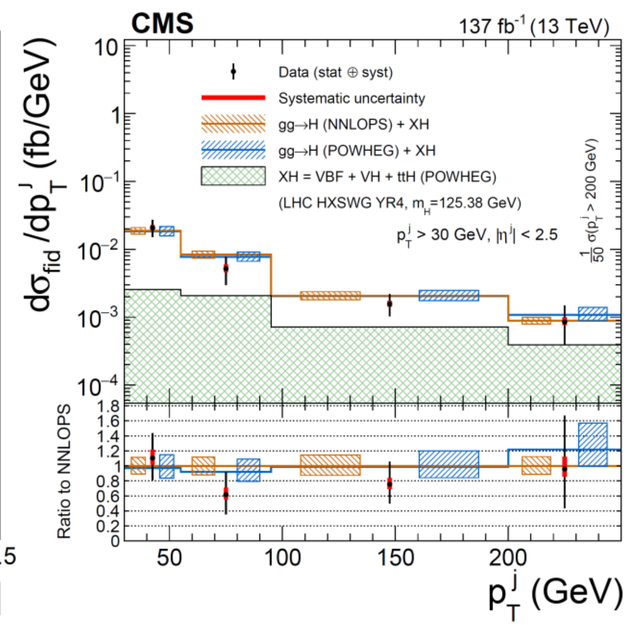

→ Fiducial cross sections are measured inclusively and in bins of p_T^H, $|y^H|$, N_{jets}, and p_T of the leading jet.

Anomalous couplings using $H \to 4\ell$

→ Analysis is submitted to PRD.

→ The analysis constrains up to five HVV, two Hgg and two Htt anomalous couplings.
→ Results for the CP measurement in Htt are combined with those using $H \to \gamma\gamma$ (CMS-HIG-19-013).
→ Constraints with multiple couplings with or without the SMEFT relations are considered in HVV couplings.

→ Most of the event selection, categorization and observables rely on the previous analysis mentioned.
→ The first level of STXS Stage 0-type categorization is used for the Hgg and Htt couplings.
→ For HVV anomalous couplings, MELA discriminant use in the VBF and hadronic VH categorization decision-making are extended for the BSM hypotheses as well. The $t\bar{t}H$ categories are dropped, and a new boosted category with 3 or fewer jets and $p_T^{4\ell} > 120$ GeV is added instead.
→ Observable usage is generalized to include binning from all relevant BSM MELA discriminants.

Anomalous couplings using $H \to 4\ell$

→ The parametrization of the amplitudes in general follow the following forms:

$$A(\mathrm{Hff}) = -\frac{m_{\mathrm{f}}}{v}\overline{\psi}_{\mathrm{f}}\left(\kappa_{\mathrm{f}} + \mathrm{i}\tilde{\kappa}_{\mathrm{f}}\gamma_5\right)\psi_{\mathrm{f}}$$

Hff couplings

$$A(\mathrm{HV_1V_2}) = \frac{1}{v}\left[a_1^{\mathrm{VV}} + \frac{\kappa_1^{\mathrm{VV}} q_{\mathrm{V1}}^2 + \kappa_2^{\mathrm{VV}} q_{\mathrm{V2}}^2}{\left(\Lambda_1^{\mathrm{VV}}\right)^2} + \frac{\kappa_3^{\mathrm{VV}} (q_{\mathrm{V1}} + q_{\mathrm{V2}})^2}{\left(\Lambda_Q^{\mathrm{VV}}\right)^2}\right] m_{\mathrm{V1}}^2 \epsilon_{\mathrm{V1}}^* \epsilon_{\mathrm{V2}}^* + \frac{1}{v} a_2^{\mathrm{VV}} f_{\mu\nu}^{*(1)} f^{*(2),\mu\nu} + \frac{1}{v} a_3^{\mathrm{VV}} f_{\mu\nu}^{*(1)} \tilde{f}^{*(2),\mu\nu}$$

HVV couplings

→ The couplings in the HVV amplitude are kept in a generic format for $V = Z, \gamma$. A similar form exists for Hgg with only the terms proportional to a_2 and a_3 remaining.
→ $SU(2) \times U(1)$ symmetry can be imposed on the amplitude by relating the couplings.
→ The relationship of these couplings to the Higgs basis can also be found in the paper.
→ The results are presented in terms of cross section or coupling fractions, or in couplings themselves.

Anomalous couplings using $H \to 4\ell$

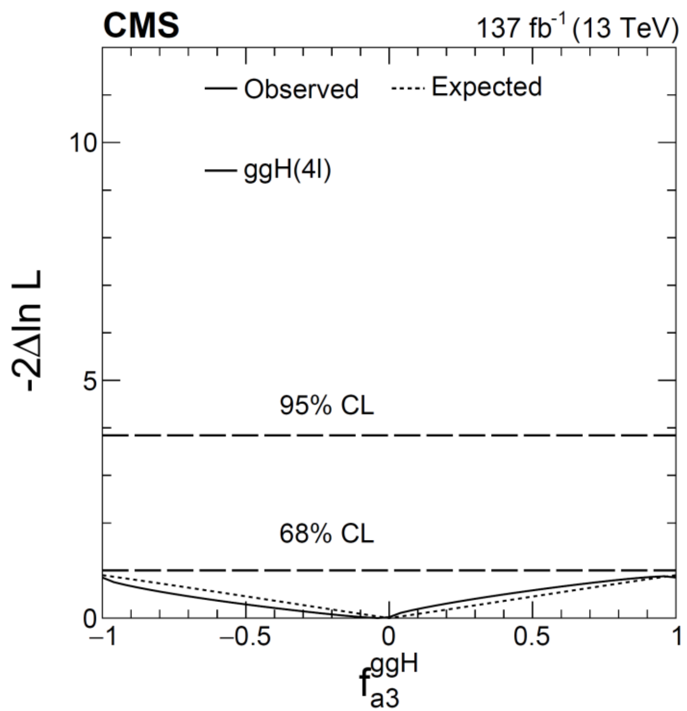

→ Constraints in ggH cross section and Htt coupling fractions are shown.

→ Most of the sensitivity comes from the $t\bar{t}H, H \to \gamma\gamma$ analysis, with 4ℓ contributing at ~1 σ level.

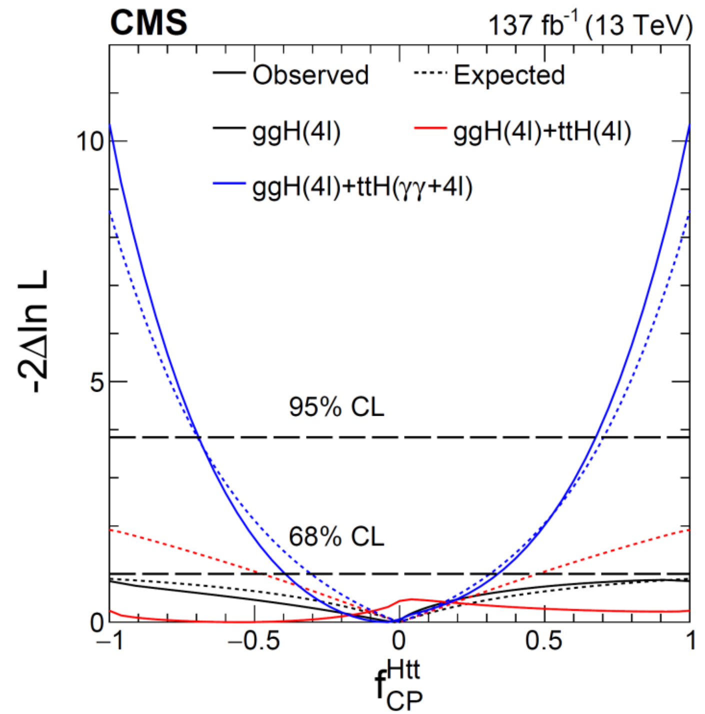

Parameter	Scenario	Observed	Expected
f_{a3}^{ggH}	ggH ($H \to 4\ell$)	$-0.04^{+1.04}_{-0.96}$ $[-1, 1]$	0 ± 1 $[-1, 1]$
f_{CP}^{Htt}	tH & $t\bar{t}$H ($H \to 4\ell$)	$\pm(0.88^{+0.12}_{-1.88})$ $[-1, 1]$	0 ± 1 $[-1, 1]$
	tH & $t\bar{t}$H ($H \to \gamma\gamma$) [26]	0.00 ± 0.33 $[-0.67, 0.67]$	0.00 ± 0.49 $[-0.82, 0.82]$
	tH & $t\bar{t}$H ($H \to 4\ell$ & $\gamma\gamma$)	0.00 ± 0.33 $[-0.67, 0.67]$	0.00 ± 0.48 $[-0.81, 0.81]$
	ggH ($H \to 4\ell$)	$-0.01^{+1.01}_{-0.99}$ $[-1, 1]$	0 ± 1 $[-1, 1]$
	ggH & tH & $t\bar{t}$H ($H \to 4\ell$)	$-0.56^{+1.56}_{-0.44}$ $[-1, 1]$	0.00 ± 0.47 $[-1, 1]$
	ggH & tH & $t\bar{t}$H ($H \to 4\ell$ & $\gamma\gamma$)	$-0.04^{+0.38}_{-0.36}$ $[-0.69, 0.68]$	0.00 ± 0.30 $[-0.70, 0.70]$

Anomalous couplings using $H \to 4\ell$

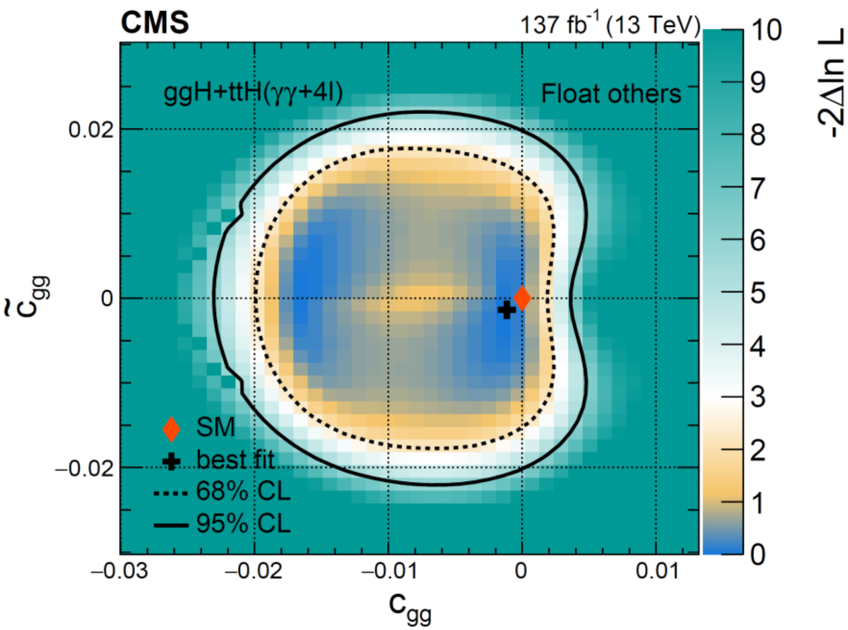

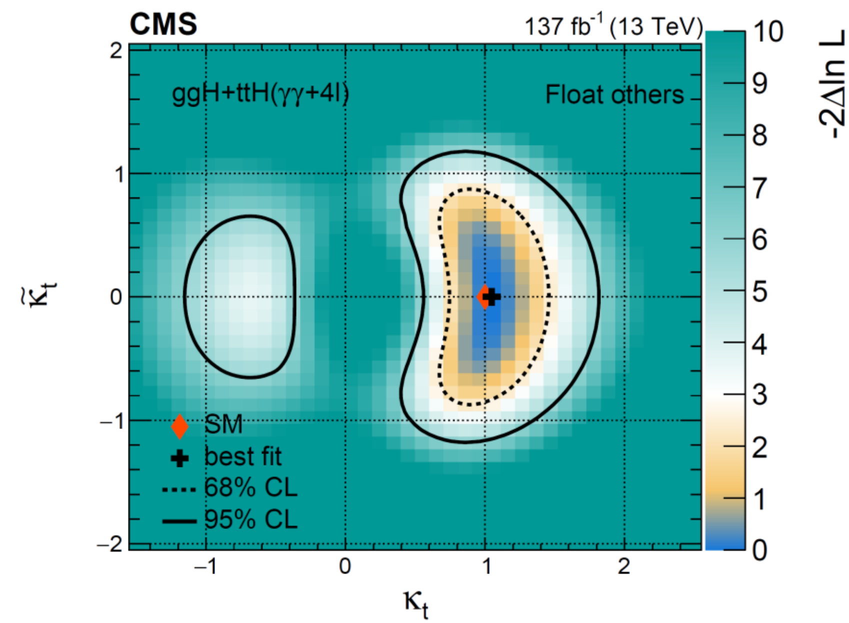

→ The constraints in Hgg and Htt couplings are also presented in 2-parameter form for the four couplings involved.

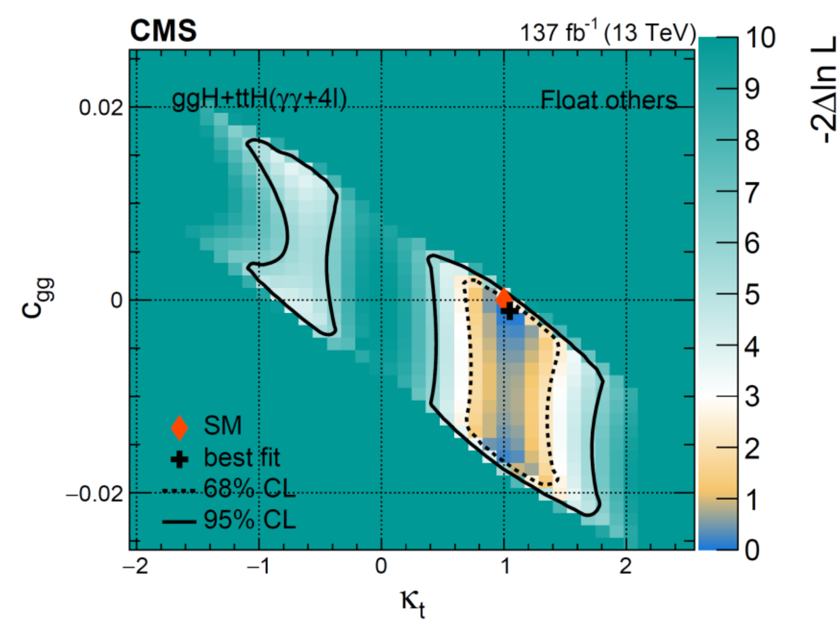

Anomalous couplings using $H \rightarrow 4\ell$

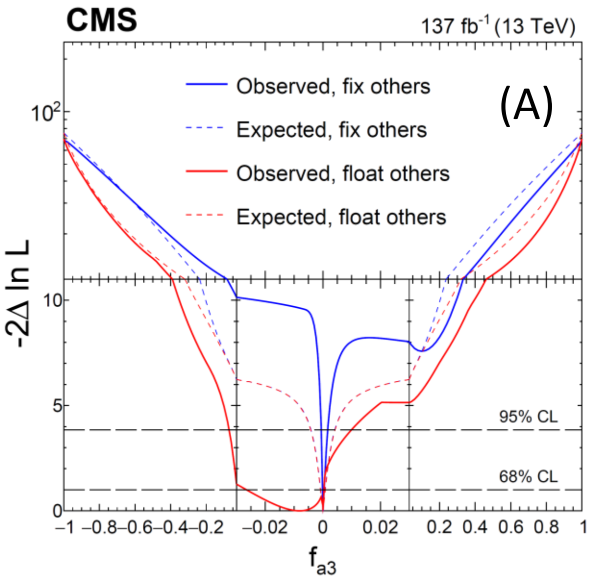

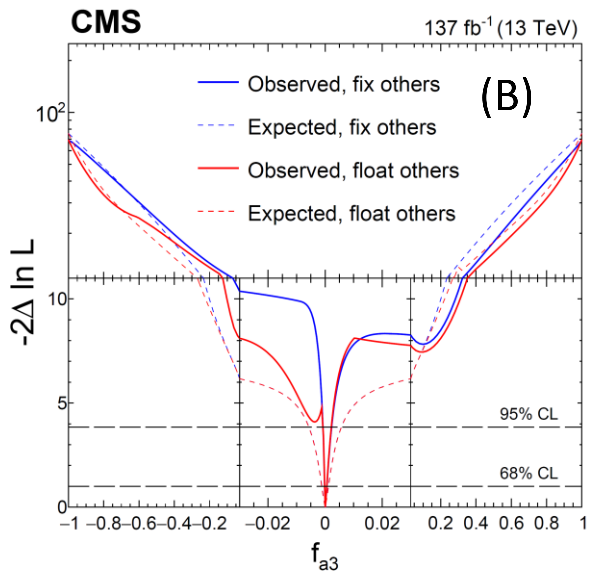

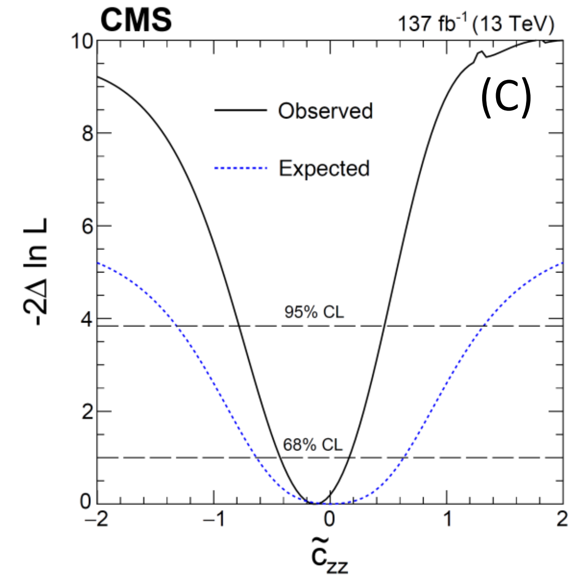

→ The constraints in HVV anomalous couplings are presented with either $a_i^{ZZ} = a_i^{WW}$ and all parameters otherwise unrelated (A), or the SMEFT relationships applied (B).

→ They are also presented in terms of the couplings in the Higgs basis, projected along each dimension (C) or in two-parameter contours (D).

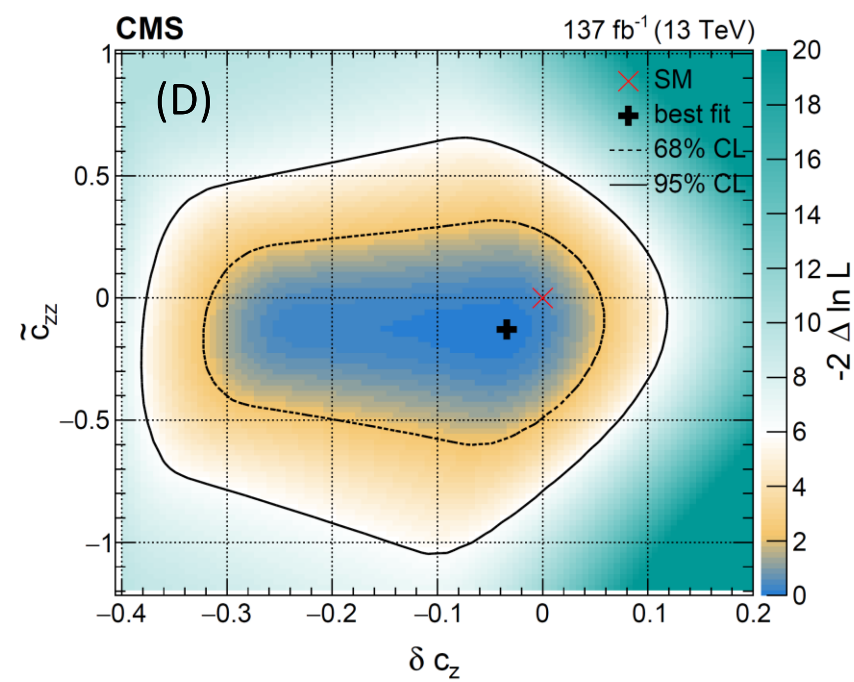

Many exciting results have become available from CMS on understanding the properties of the Higgs boson.

Excellent progress is made in exploiting the most out of the kinematic information in the events.

Stay tuned for more exciting results in the upcoming months!

Thank you!

Back-up

Fiducial cross sections using $H \rightarrow \tau\tau$

Generated bin	σ_{fid}^{SM} (fb)	Unregularized μ	Regularized μ	σ_{fid}^{obs} (fb)
$N_{jets} = 0$	168 ± 15	$1.26^{+0.51}_{-0.50}$	$1.25^{+0.46}_{-0.48}$	210^{+86}_{-84}
$N_{jets} = 1$	138 ± 15	$0.99^{+0.30}_{-0.30}$	$1.00^{+0.28}_{-0.27}$	138^{+39}_{-37}
$N_{jets} = 2$	71.1 ± 9.4	$0.87^{+0.26}_{-0.25}$	$0.84^{+0.22}_{-0.22}$	$59.7^{+15.6}_{-15.6}$
$N_{jets} = 3$	21.1 ± 3.2	$0.48^{+0.50}_{-0.48}$	$0.58^{+0.36}_{-0.35}$	$12.2^{+7.6}_{-7.4}$
$N_{jets} \geq 4$	10.2 ± 1.7	$0.63^{+0.53}_{-0.50}$	$0.57^{+0.46}_{-0.45}$	$5.81^{+4.69}_{-4.59}$
$p_T^H < 45\,\text{GeV}$	209 ± 16	$0.35^{+0.49}_{-0.50}$	$0.11^{+0.43}_{-0.44}$	$23.0^{+89.9}_{-92.0}$
$45 < p_T^H < 80\,\text{GeV}$	81.7 ± 7.0	$-0.40^{+0.71}_{-0.71}$	$0.34^{+0.46}_{-0.45}$	$27.8^{+37.6}_{-36.8}$
$80 < p_T^H < 120\,\text{GeV}$	48.5 ± 4.7	$2.00^{+0.68}_{-0.66}$	$1.28^{+0.43}_{-0.40}$	$62.1^{+20.9}_{-19.4}$
$120 < p_T^H < 200\,\text{GeV}$	45.4 ± 5.9	$0.95^{+0.34}_{-0.33}$	$1.18^{+0.26}_{-0.26}$	$53.6^{+11.8}_{-11.8}$
$200 < p_T^H < 350\,\text{GeV}$	20.1 ± 4.9	$1.17^{+0.46}_{-0.37}$	$1.18^{+0.41}_{-0.36}$	$23.7^{+8.2}_{-7.2}$
$350 < p_T^H < 450\,\text{GeV}$	2.49 ± 0.62	$1.79^{+0.93}_{-0.72}$	$1.68^{+0.67}_{-0.59}$	$4.18^{+1.67}_{-1.47}$
$p_T^H > 450\,\text{GeV}$	0.823 ± 0.209	$1.82^{+1.19}_{-0.94}$	$2.00^{+1.02}_{-0.85}$	$1.65^{+0.84}_{-0.70}$
$N_{jets} = 0$	168 ± 15	$1.20^{+0.52}_{-0.52}$	$1.11^{+0.50}_{-0.50}$	186^{+84}_{-84}
$30 < p_T^{j_1} < 60\,\text{GeV}$	108 ± 11	$0.13^{+0.46}_{-0.46}$	$0.24^{+0.42}_{-0.41}$	$25.9^{+45.4}_{-44.3}$
$60 < p_T^{j_1} < 120\,\text{GeV}$	81.1 ± 7.5	$0.62^{+0.29}_{-0.29}$	$0.60^{+0.27}_{-0.27}$	$48.7^{+21.9}_{-21.9}$
$120 < p_T^{j_1} < 200\,\text{GeV}$	34.9 ± 4.2	$1.15^{+0.28}_{-0.27}$	$1.13^{+0.26}_{-0.25}$	$39.4^{+9.1}_{-8.7}$
$200 < p_T^{j_1} < 350\,\text{GeV}$	13.5 ± 3.0	$1.02^{+0.39}_{-0.35}$	$1.06^{+0.38}_{-0.34}$	$14.3^{+5.1}_{-4.6}$
$p_T^{j_1} > 350\,\text{GeV}$	2.38 ± 0.57	$1.32^{+0.76}_{-0.65}$	$1.30^{+0.72}_{-0.63}$	$3.09^{+1.71}_{-1.50}$

→ 'Regularized' refers to a Tikhonov procedure to mitigate statistical fluctuations in unfolding.

→ Second occurrence of $N_{jets} = 0$ uses fitting in p_T^h bins.

Fiducial region for $H \rightarrow 4l$

Requirements for the $\mathrm{H} \rightarrow 4\ell$ fiducial phase space	
Lepton kinematics and isolation	
Leading lepton p_{T}	$p_{\mathrm{T}} > 20\,\mathrm{GeV}$
Next-to-leading lepton p_{T}	$p_{\mathrm{T}} > 10\,\mathrm{GeV}$
Additional electrons (muons) p_{T}	$p_{\mathrm{T}} > 7(5)\,\mathrm{GeV}$
Pseudorapidity of electrons (muons)	$\lvert\eta\rvert < 2.5\ (2.4)$
Sum of scalar p_{T} of all stable particles within $\Delta R < 0.3$ from lepton	$< 0.35 p_{\mathrm{T}}$
Event topology	
Existence of at least two same-flavor OS lepton pairs, where leptons satisfy criteria above	
Inv. mass of the Z_1 candidate	$40 < m_{\mathrm{Z}_1} < 120\,\mathrm{GeV}$
Inv. mass of the Z_2 candidate	$12 < m_{\mathrm{Z}_2} < 120\,\mathrm{GeV}$
Distance between selected four leptons	$\Delta R(\ell_i, \ell_j) > 0.02$ for any $i \neq j$
Inv. mass of any opposite sign lepton pair	$m_{\ell^+\ell'^-} > 4\,\mathrm{GeV}$
Inv. mass of the selected four leptons	$105 < m_{4\ell} < 140\,\mathrm{GeV}$